

Experimental characterisation of as-built and retrofitted timber-masonry connections under monotonic, cyclic and dynamic loading

Mirra, Michele; Ravenshorst, Geert; de Vries, Peter; Messali, Francesco

DOI

[10.1016/j.conbuildmat.2022.129446](https://doi.org/10.1016/j.conbuildmat.2022.129446)

Publication date

2022

Document Version

Final published version

Published in

Construction and Building Materials

Citation (APA)

Mirra, M., Ravenshorst, G., de Vries, P., & Messali, F. (2022). Experimental characterisation of as-built and retrofitted timber-masonry connections under monotonic, cyclic and dynamic loading. *Construction and Building Materials*, 358, Article 129446. <https://doi.org/10.1016/j.conbuildmat.2022.129446>

Important note

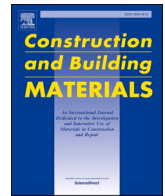
To cite this publication, please use the final published version (if applicable).
Please check the document version above.

Copyright

Other than for strictly personal use, it is not permitted to download, forward or distribute the text or part of it, without the consent of the author(s) and/or copyright holder(s), unless the work is under an open content license such as Creative Commons.

Takedown policy

Please contact us and provide details if you believe this document breaches copyrights.
We will remove access to the work immediately and investigate your claim.



Experimental characterisation of as-built and retrofitted timber-masonry connections under monotonic, cyclic and dynamic loading

Michele Mirra^{a,*}, Geert Ravenshorst^a, Peter de Vries^a, Francesco Messali^b

^a Department of Engineering Structures, Section of Biobased Structures and Materials, Delft University of Technology, Stevinweg 1, 2628 CN Delft, the Netherlands

^b Department of Materials, Mechanics, Management & Design, Section of Applied Mechanics, Delft University of Technology, Stevinweg 1, 2628 CN Delft, the Netherlands

ARTICLE INFO

Keywords:

Timber-masonry connections
Damage
Retrofitting
Seismic Rehabilitation

ABSTRACT

In the province of Groningen (NL), where human-induced earthquakes take place due to gas extraction, a large part of the building stock is composed of brick masonry walls and timber diaphragms. In this framework, timber-masonry connections play a crucial role in the global seismic response of the buildings, but their properties and structural behaviour have not been investigated yet for the Dutch context. This work describes the experimental campaign conducted at Delft University of Technology to characterize as-built and strengthened timber-masonry connections. The joints were tested under either quasi-static monotonic, cyclic or dynamic loading, to analyse the effect of an induced earthquake signal on the connections' response in terms of strength, stiffness and damage evolution. The obtained test results provided more insight into the capacity and properties of existing connections, and useful knowledge on the effectiveness of the tested retrofitting methods.

1. Introduction

1.1. Background

Historical or existing buildings are often composed of brick or stone masonry walls, and timber floors and roofs. When earthquakes occur, the interaction among these structural components is essential to avoid collapse or excessive damage to the constructions. In this framework, a crucial role is played by the connections between horizontal and vertical structural elements: this is especially true when considering existing buildings not designed to resist seismic actions, because connections often represent the most critical detail to allow the structure to develop the desired box behaviour.

An example of such a situation is noticeable in the province of Groningen, in the northern part of the Netherlands, where human-induced earthquakes have started to take place due to gas extraction [1]. These events were unknown until recently: the gas extraction started in 1963, and earthquakes have occurred since the early '90s, with a progressive increase in the number of events and in their intensity. Up to now, the highest magnitude was experienced near Hui-zinge in 2012, and was equal to 3.6 on the Richter scale. The current building stock has not been designed to withstand seismic actions:

nearly 50 % of the buildings are composed of unreinforced single-leaf or double-wythe brick masonry walls, and timber floors and roofs. The slenderness of the walls (both in-plane and out-of-plane) and the low in-plane stiffness of the diaphragms, due to small-size timber structural elements, make existing buildings very vulnerable against earthquakes. So far, the damage was limited to cracks and did not lead to total collapse of the houses. However, when earthquakes take place with much larger intensities, which may occur according to probabilistic calculations, then way more extensive damage can be foreseen.

Therefore, extensive experimental campaigns were arranged to characterize the material properties of existing masonry walls and timber diaphragms. These detailed analyses enabled the accurate replication of both masonry [1–5] and timber [6] for testing as-built full-scale structural components representative for the actual building stock, and provided more insight into their material properties and structural response to horizontal loading. After this first step, seismic strengthening measures were defined as well [7–10].

Within this comprehensive study, one of the main vulnerabilities of existing buildings appeared to be the presence of relatively poor connections between timber floors and masonry walls. For the purpose of seismic assessment, the characterization of existing joints was necessary; furthermore, an analysis of retrofitting solutions was carried out as well.

* Corresponding author.

E-mail addresses: M.Mirra@tudelft.nl (M. Mirra), G.J.P.Ravenshorst@tudelft.nl (G. Ravenshorst), P.A.deVries@tudelft.nl (P. de Vries), F.Messali@tudelft.nl (F. Messali).

<https://doi.org/10.1016/j.conbuildmat.2022.129446>

Received 4 February 2021; Received in revised form 6 October 2022; Accepted 12 October 2022

Available online 23 October 2022

0950-0618/© 2022 The Author(s). Published by Elsevier Ltd. This is an open access article under the CC BY license (<http://creativecommons.org/licenses/by/4.0/>).

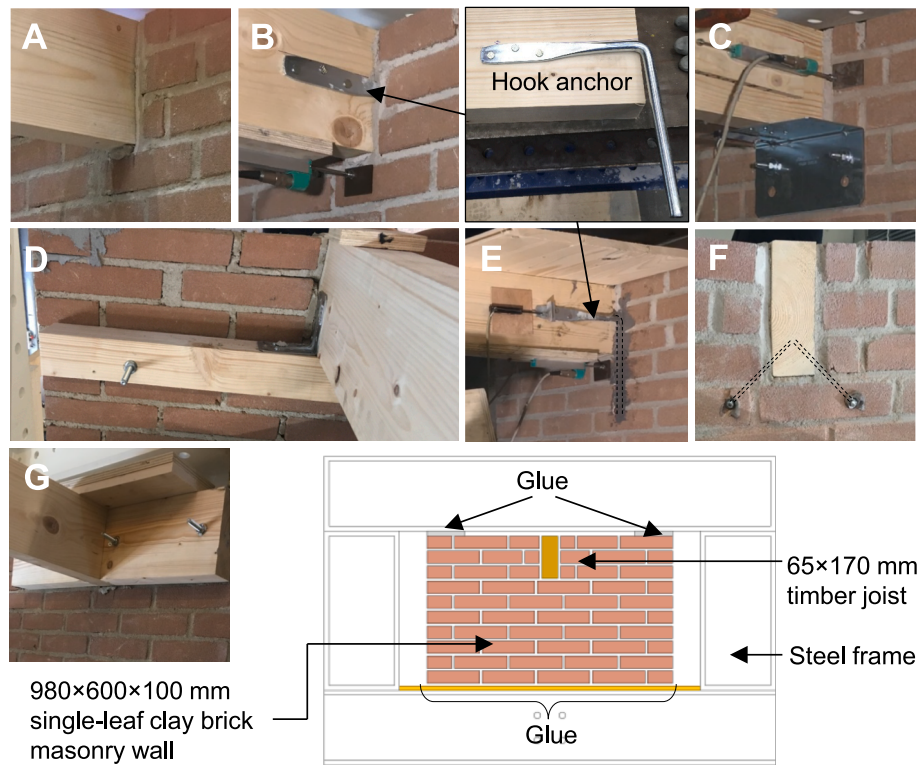


Fig. 1. Overview on the 7 tested configuration: as-built with mortar pocket (A); as-built with hook anchor (B); strengthened with steel angle (C); strengthened with additional joist and steel brackets (D); strengthened with hook anchor glued into the wall (E); strengthened with two screws glued into the wall (F); strengthened with timber blocks (G); the principle and the description of a typical sample are also shown.

Thus, a full-scale experimental campaign was arranged and conducted at Delft University of Technology, focusing on the response of as-built and strengthened timber-masonry connections.

For the US context, results of tests on compact samples representing as-built timber-masonry connections were summarized in [11]. The specimens consisted of either a joist embedded in a masonry pocket with mortar, or the same configuration with the additional presence of a nailed anchor. Quasi-static monotonic or cyclic, and dynamic cyclic tests were performed. In the latter loading protocol, ten high-frequency cycles at the same amplitude were repeated, and the signal was progressively scaled to describe the connections' full response. The samples were very compact, so that the response of the whole wall portion around the joint could not be captured, while the frictional response and the failure modes of nails and anchors were thoroughly characterized. Due to the specific configuration of the connections, the detected response was asymmetric: when pulling the joist, only the nails and the anchor could resist the load, while in the opposite direction also the masonry bricks played a role.

As-built and retrofitted wall-to-floor connections with Portuguese features were studied in [12,13], by performing pull-out and cyclic tests on full-scale samples. The proposed strengthening solution consisted of a tie rod anchoring the wall to the joist through a steel angle. Several elements of the connection were tested, and their various failure modes were identified and discussed. Besides, the large dimensions of the tested samples enabled to account for the effect of the masonry portion around the floor joist, as well as the influence of the wall thickness.

Finally, in-situ monotonic tests on two unreinforced masonry buildings in New Zealand were performed and their outcomes discussed in [14]: plate anchor and timber blocking connection types were studied, and failure modes were thoroughly discussed. Timber joist splitting was the most commonly observed failure mode for the plate anchor connection, showing that its capacity was mainly governed by the condition of the timber joist or the characteristics of the wall. Instead,

timber blocking connection showed great ductility, but in general less capacity compared to plate anchor one.

1.2. Research objectives and approach

This work describes the experimental campaign conducted at Delft University of Technology for characterizing two as-built and five strengthened configurations of timber-masonry connections. The knowledge provided by previous research studies was used to design the current campaign, which was, on the other hand, focused on the specific Groningen situation. Therefore, the size of the samples was defined in such a way that it was possible to study the behaviour of the portion of wall around the timber joist; additionally, dynamic tests with a signal of an induced Groningen earthquake were performed, besides the usual quasi-static monotonic and cyclic ones. This enabled the characterization of the connections' response, as well as the damage on the masonry walls, under this specific seismic loading.

The first objective of the research study is to analyse the response of as-built joints, as a starting point for the subsequent definition of retrofitting solutions selected and designed together with local consultants. Within five strengthening methods selected, three of them privileged ductility and energy dissipation, while two options were developed for providing high strength and stiffness. The second objective of the study is to compare the damage caused on masonry by an induced earthquake loading with the one observed after quasi-static cyclic tests and, for one retrofitted solution, also after applying a tectonic earthquake signal. Finally, this study aims to discuss and compare the performance of the tested connections in terms of strength, stiffness, energy dissipation and damage on masonry.

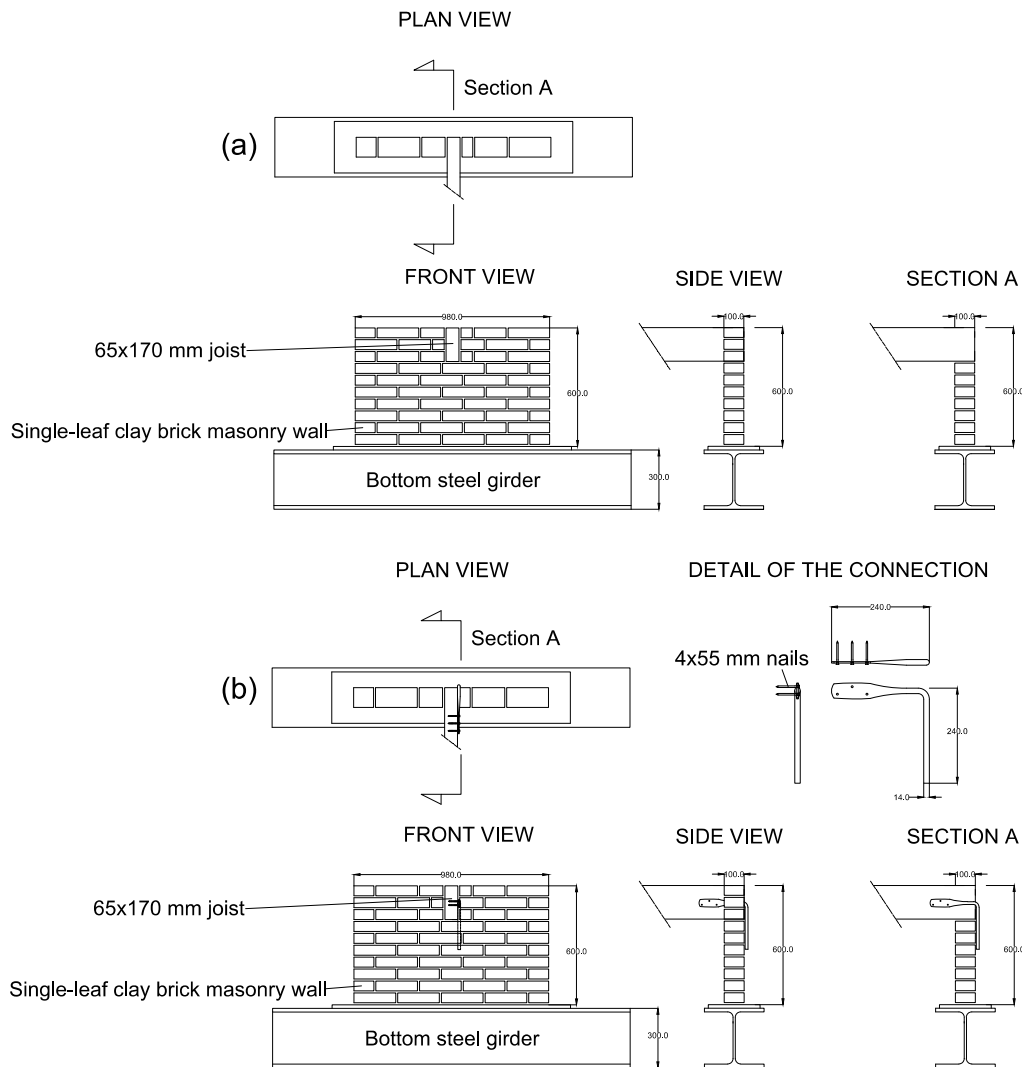


Fig. 2. Detailed representation of configurations A (a), B (b), C (c), D (d), E (e), F (f), G (g).

2. Materials and methods

2.1. Materials

In this experimental campaign, the connection of a timber joist with a single-leaf clay brick masonry wall was investigated. This situation, for the Dutch context, is representative for the inner leaf of a cavity wall structure at roof level, or for a gable. Both constitute a very weak part of existing buildings, due to the absence of ongoing masonry on top and the frequent presence of low-quality or damaged masonry.

The specimens consisted of 980×600 mm masonry wall elements. A 65×170 mm timber joist was inserted orthogonally to the wall, with a length of approximately 1600 mm (Fig. 1). The masonry walls were glued at the bottom and at the two top corners, to ensure that the behaviour of the joist-masonry connection was studied, accounting for the portion of wall around it.

In total, seven configurations were studied (Figs. 1-2), two as-built ones (A, B) and five strengthened ones (C-G). Seven samples were tested for each option, as described in section 2.2.1, resulting in a total number of 49 tests. The two as-built connections consisted of a simple masonry pocket with mortar (A, Fig. 2a), and of a typical Dutch joint realized with a $240 \times 240 \times 14$ mm hook anchor (B, Fig. 2b) fastened to the joist with three 4×55 mm nails. In the Groningen area, these

connections are widely present, and can be found in detached houses (both configurations) and terraced houses (mainly configuration B). In single-leaf walls (100 mm thickness), this hook anchor is behind the leaf (see Figs. 1-2), while for double-wythe walls (210 mm thickness) it is masoned in them. The former is the weakest connection type, thus the single-leaf configuration was tested.

Strengthening options C and D were tested by reusing the specimens realized for the as-built connections, so that they were in fact retrofitted samples. The first proposed retrofitting solution (C, Fig. 2c) consisted of a steel angle fastened to the joist with four 5×60 mm screws and to the masonry with two 10×95 mm mechanical anchors. This strengthening option was applied on the tested samples representing the as-built masonry pocket connection (A), because the weakness of the joist-masonry interface prevented the masonry from being damaged. Retrofitting method D (Fig. 2d) was, instead, developed for masonry damaged around the joist, which may also be representative for low-quality masonry at the top of a wall. Therefore, for this option a further 80×80 mm joist was attached with 10×165 mm anchors only to sound masonry below the existing joist, and then fastened to it by means of two $90 \times 90 \times 3$ mm steel brackets and four 5×60 mm screws for each of them. In this case, the samples from configuration B were reused, because the presence of the hook anchor was expected to damage the masonry around the joists while testing, as it happened. It should be noted that,

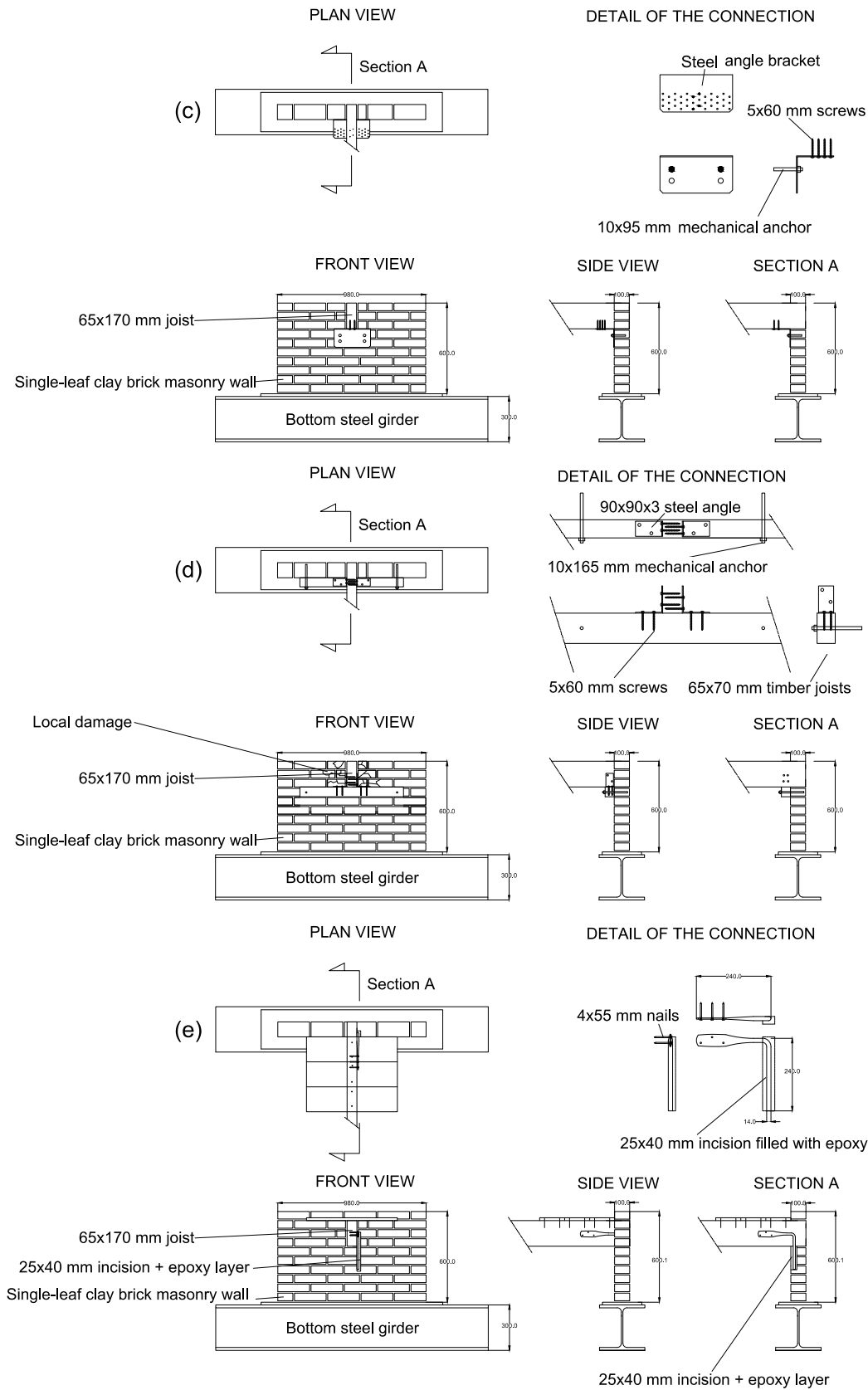


Fig. 2. (continued).

before strengthening these samples, the hook anchor was disconnected from the timber joist.

Strengthening options E, F and G were tested on newly-built walls.

Configuration E (Fig. 2e) consisted of a 240 × 240 × 14 mm hook anchor fastened to the joist with three 4 × 55 mm nails and then glued with epoxy to a 25 × 40 × 240 mm incision realized on the front side of the

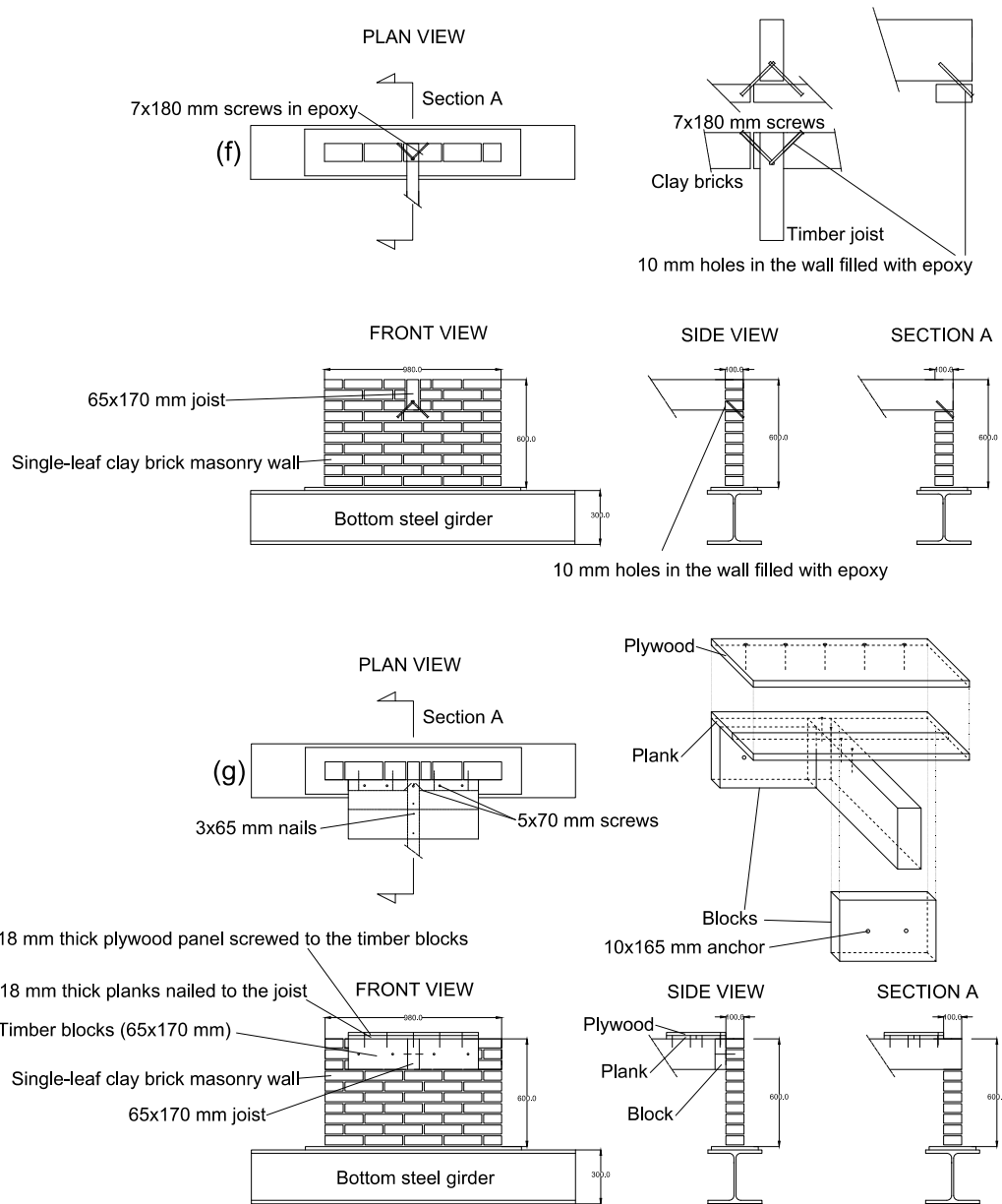


Fig. 2. (continued).

wall. Retrofitting method F (Fig. 2f) was realized by connecting the joist to the wall with two inclined 7×180 mm screws. These were inserted into the joist after drilling holes of 10 mm diameter in the masonry and filled with injected epoxy: the screws were, therefore, partly embedded in the glue, and partly inserted in the joist. This intervention can be realized from the outside of a building: directly, when the measure is applied to gables, or by removing a limited number of bricks from the outer leaf, for the inner leaf of a cavity wall. While for configurations E and F the goal was the achievement of a much higher strength and stiffness compared to the as-built situation, even if renouncing to ductility, for configuration G (Fig. 2g) this latter aspect was privileged. This option was also part of a floor strengthening intervention presented in [6], and was realized with 65×170 mm timber blocks placed on both sides of the joist (in practice they would be positioned between each couple of joists). The blocks were firstly fixed to the existing joist by means of two 5×70 mm screws drilled at an angle of 45 degrees, and then fastened to the masonry with two 10×165 mm mechanical anchors each. However, since this intervention would in practice involve

also the timber diaphragm, it was important to recreate the same conditions: hence, besides the presence of a 18×165 mm plank, fixed to the joist with two 3×65 mm nails, also an additional 18-mm-thick plywood panel overlay was fastened to the plank and inside the blocks with five 5×70 mm screws.

All timber structural elements were made of C24 timber [15], namely spruce (*Picea Abies*). For characterizing the masonry and the mechanical anchors, specific companion tests were performed, as reported in section 2.2.1; the results in terms of material properties are summarized in section 3.1.

2.2. Methods

2.2.1. Companion tests on timber, masonry, and mechanical anchors

The main material properties determined for timber elements were density, moisture content and modulus of elasticity. The density was measured by weighing the samples and dividing the weight by their volume. The moisture content was derived according to EN 13183 [16];

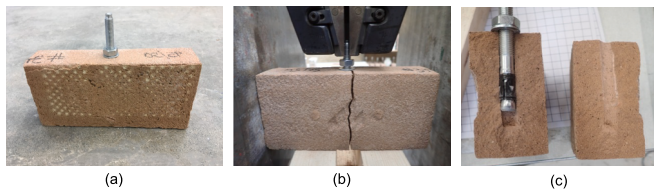


Fig. 3. Example of specimen prepared for testing pull-out and shear strength of mechanical anchors in masonry: sample before (a) and after testing (b); specimen opened along its crack after removal from test setup (c).

the modulus of elasticity was dynamically measured [17].

With regard to masonry, several relevant material properties were determined, and namely compressive and flexural strength of mortar according to EN 1015-11:1999 [18]; density of masonry; compressive strength, elastic modulus, Poisson ratio and peak strain in compression according to EN 1052-1:1998 [19]; flexural bond strength according to EN1052-5:2002 [20]; shear strength and friction coefficient according

to EN 1052-3:2002 [21].

Besides, since standard pull-out and shear strength values for anchors are commonly reported in producers' catalogues with reference to C20/25 concrete [22], the adopted mechanical anchors were tested to assess these properties for masonry bricks, following the testing protocol of EN 846-5:2012 [23]. For both pull-out and shear tests, a rate of 0.1 mm/s was applied and the anchors were fastened to the centre of a brick with a penetration length of 70 mm. The pull-out and shear strength and stiffness values are provided in Section 3.1 along with the other material properties of timber and masonry. A specimen before and after the test is shown in Fig. 3.

2.2.2. Test setup and measurement plan

Fig. 4a shows a 3D view of the designed test setup: it was composed of a static part, fastened to the laboratory floor, and a moving part on top of which each specimen was placed. Sliding of the moving part was ensured by rollers, while its possible rotations were prevented by plates and wheels close to the rollers. In this way, it was possible to enable only the axial horizontal displacements transmitted by the actuator,

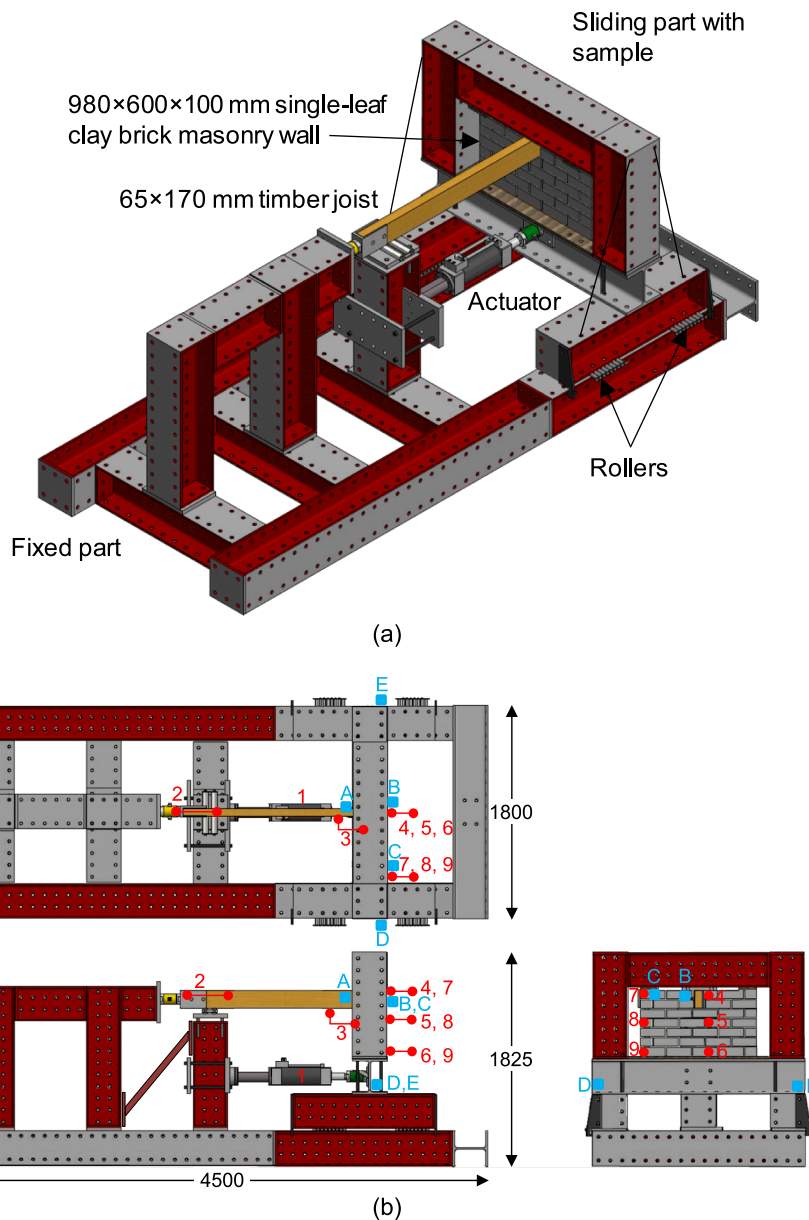


Fig. 4. Test setup (a) and measurement plan (b).

Table 1
Overview on the performed tests and adopted nomenclature.

Configuration	Description	Test types	Specimen name(s)
A	As-built joist-wall connection. Clay bricks single-leaf wall with the joist in a mortar pocket.	1 quasi-static monotonic test	A-M-1
		3 quasi-static cyclic tests	A-QS-1, A-QS-2, A-QS-3
		3 high-frequency dynamic tests	A-HFD-1, A-HFD-2, A-HFD-3
B	As-built joist-wall connection. Clay bricks single-leaf wall with hook anchor.	1 quasi-static monotonic test	B-M-1
		3 quasi-static cyclic tests	B-QS-1, B-QS-2, B-QS-3
		3 high-frequency dynamic tests	B-HFD-1, B-HFD-2, B-HFD-3
C	Strengthening option for joist-wall connections in sound masonry. Configuration A retrofitted with an angle bracket screwed to the joist and anchored to the wall.	1 quasi-static monotonic test	C-M-1
		3 quasi-static cyclic tests	C-QS-1, C-QS-2, C-QS-3
		3 high-frequency dynamic tests	C-HFD-1, C-HFD-2, C-HFD-3
D	Strengthening option for joist-wall connections in damaged or low-quality masonry. Configuration B retrofitted with a further joist anchored to sound masonry and fixed to the existing joist with steel brackets. The hook anchor is disconnected.	1 quasi-static monotonic test	D-M-1
		3 quasi-static cyclic tests	D-QS-1, D-QS-2, D-QS-3
		3 high-frequency dynamic tests	D-HFD-1, D-HFD-2, D-HFD-3
E	Clay bricks single-leaf wall. Strengthening with an hook anchor nailed to the joist and glued to the wall after being placed in a previously realised incision on it.	1 quasi-static monotonic test	E-M-1
		3 quasi-static cyclic tests	E-QS-1, E-QS-2, E-QS-3
		3 high-frequency dynamic tests	E-HFD-1, E-HFD-2, E-HFD-3
F	Clay bricks single-leaf wall. Strengthening with two inclined screws inserted into the joist after drilling in the masonry proper holes, filled with epoxy.	1 quasi-static monotonic test	F-M-1
		3 quasi-static cyclic tests	F-QS-1, F-QS-2, F-QS-3
		3 high-frequency dynamic tests	F-HFD-1, F-HFD-2, F-HFD-3
G	Clay bricks single-leaf wall. Strengthening with timber blocks placed on both sides of the existing joist, screwed to it and to timber floor, and anchored to the wall.	1 quasi-static monotonic test	G-M-1
		3 quasi-static cyclic tests	G-QS-1, G-QS-2, G-QS-3
		3 high-frequency dynamic tests	G-HFD-1, G-HFD-2, G-HFD-3

connecting the static part of the setup to the bottom beam on which each wall was built. Every sample was confined by a steel frame, to guarantee its stability; this frame was also furtherly connected with bracings to the edges of the two horizontal steel beams sliding on rollers, in order to ensure an optimal stability against possible vibrations. A weight of 100 kg was hanged with a rope at mid span on the wooden joist, to represent the loads acting on that portion of floor around the connection in practice (0.5 kN).

In order to guarantee an effective action of the hydraulic actuator, the column on which it was clamped was furtherly braced to the bottom frame. This bracing, not shown in Fig. 4a, is represented in Fig. 4b. As can be noticed, the displacements were not imposed directly to the joist, but to the bottom part of the wall. In this way, it was possible to use a single versatile setup with a realistic load application for all the three test typologies. In order to record the force transferred by the connections, a load cell was connected to the timber joist and to a stiff frame in the rear part of the setup.

Fig. 4b shows the adopted measurement plan: for monotonic and quasi-static tests, potentiometers were used (sensors 1–9). Only for high frequency dynamic tests, accelerometers were also placed (sensors A-E, with maximum capacity 2.5 g), to have a more accurate detection of the connection's response due to a sudden solicitation. Sensor 3 was the most meaningful source of information, because it measured the relative displacement between joist and wall. Sensors 4 to 9 recorded the out-of-plane displacement of the wall, and they were fastened to a wooden structure clamped in front of it. Furthermore, for strengthened configurations a larger number of sensors were adopted, to detect also local mechanisms, such as deformation of steel angle or brackets, screws' displacement, and sliding between timber elements.

The following sign convention was adopted:

- A positive displacement sign corresponds to a pulling force on the connection (and therefore to a pushing action of the actuator at the sample's bottom);
- A negative displacement sign corresponds to a pushing force on the connection (and therefore to a pulling action of the actuator at the sample's bottom).

Besides the adopted sensors, for the two stiffest configurations (E and F), for which small displacements were expected, also digital image correlation (DIC) technique was employed, to have a complete coverage of the samples' response. The DIC system consisted of two cameras, placed at 700 mm from the wall's front side, having a resolution of 4096 × 3000 pixels each, and a frame rate up to 100 fps: this enabled the detection of out-of-plane and three-dimensional mechanisms, also for dynamic tests. A random pattern with matt black colour was applied to the front side of the walls for detecting their displacements.

2.2.3. Test types

For each configuration, seven tests were performed under displacement control, and namely-one monotonic test (M) to determine the ultimate displacement, three quasi-static reversed-cyclic tests (QS), and three high-frequency dynamic tests (HFD). Table 1 reports an overview of the performed tests and the adopted nomenclature.

Monotonic and quasi-static reversed-cyclic tests were performed according to ISO 16670 [24]. Therefore, after determining the ultimate displacement of each configuration with monotonic tests, the amplitudes of the cycles were defined accordingly, and each cycle consisted of three runs in agreement with the standard. A rate of 0.3 mm/s was adopted.

Dynamic tests were performed by applying to the specimen a specific high-frequency signal generated by the hydraulic actuator. These tests were performed not only to compare the results with quasi-static tests' ones and to check their reliability, but also to investigate the effect of a sudden signal, similar to the typical short-duration shocks observed in Groningen, to the joints. The input dynamic signal was chosen starting from shaking table tests on typical Dutch buildings: it consisted of a recorded displacement history of a timber-masonry connection during a shaking table test performed at EUCENTRE [25], and it is shown in Fig. 5 along with the performed runs. This reference signal was induced in the joint by an input accelerogram corresponding to 133 % of the estimated reference response spectrum of Groningen region, for a 2475 years return period [25]. It should be noticed that such an earthquake has never occurred, therefore no comparison with damage observed in practice until recently can be made.

The dynamic tests were conducted starting from a very small-amplitude signal (2.5 % of the reference one from [25]), and then repeating it, progressively increasing the amplitude until collapse (or maximum applied displacement) was reached. In this way, a test sequence based on progressive damage accumulation could be applied. It should be noticed that for as-built configurations A and B the largest reached amplitude was 150 mm, while for strengthened configurations C to G displacements up to 240 mm were imposed, corresponding to the

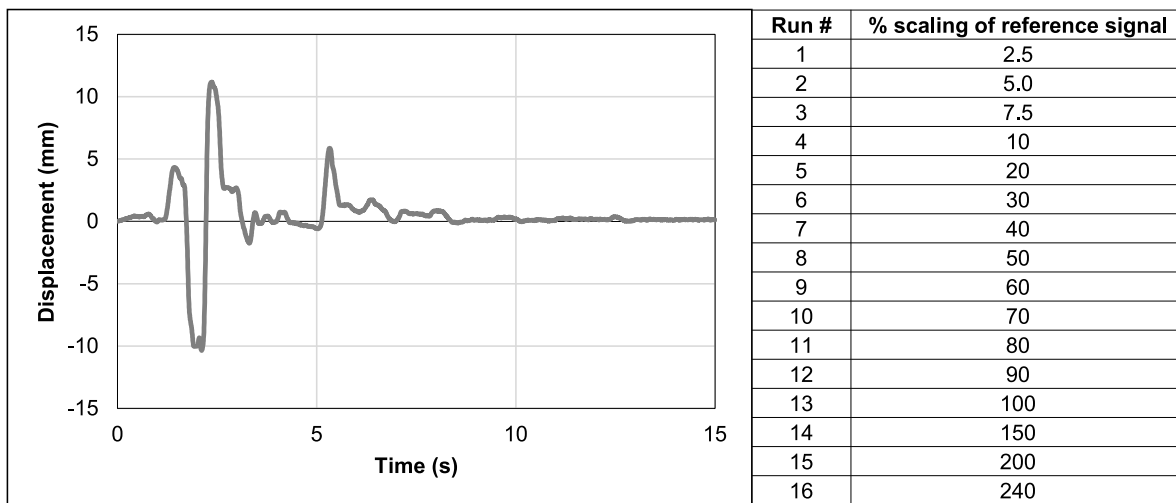


Fig. 5. Adopted signal for HFD tests and performed runs; for as-built configurations A and B the maximum reached amplitude was 150 % of the reference signal, linked to a 2475 years return period.

Table 2
Relevant material properties of timber elements.

Material property	Number of tests	Mean value	Coefficient of variation
Density (kg/m ³)	21	477	0.11
Dynamic modulus of elasticity (MPa)	21	12,216	0.16
Moisture content (%)	36	13	0.06

Table 3
Relevant material properties of masonry.

Material property	Reference standard	Number of tests	Mean value	Coefficient of variation
Compressive strength of mortar (MPa)	EN 1015-11:1999 [18]	48	4.84	0.11
Flexural strength of mortar (MPa)	EN 1015-11:1999 [18]	24	2.05	0.15
Density of masonry (kg/m ³)	-	43	1602	0.05
Compressive strength of masonry (MPa)	EN 1052-1:1998 [19]	6	11.87	0.09
Elastic modulus of masonry (MPa)	EN 1052-1:1998 [19]	6	3278	0.17
Poisson ratio of masonry	EN 1052-1:1998 [19]	6	0.15	0.17
Peak strain in compression (%)	EN 1052-1:1998 [19]	6	4.31	0.12
Flexural bond strength (MPa)	EN 1052-5:2002 [20]	28	0.11	0.51
Shear strength (MPa)	EN 1052-3:2002 [21]	18	0.15	0.10
Friction coefficient	EN 1052-3:2002 [21]	18	0.78	0.10

maximum actuator's capacity. The reduced amplitude for as-built connections was adopted in order not to excessively damage the samples, enabling their reuse afterwards for testing configuration C and D.

Table 4
Pull-out and shear strength and stiffness of mechanical anchors; as an indication, the characteristic values from the producer with reference to cracked C20/25 concrete and seismic action category C1 are reported [22].

Test type	Property	Number of tests	Mean value	Coefficient of variation	Producer's value for cracked C20/25 concrete (seismic action category C1)
Pull-out	Pull-out strength (kN)	7	6.14	0.19	8.0
	Initial stiffness (kN/mm)	7	8.27	0.32	8.33
Shear	Shear strength (kN)	8	2.68	0.16	17.0
	Initial stiffness (kN/mm)	8	1.19	0.40	2.7

3. Experimental results

3.1. Material properties of timber, masonry, and mechanical anchors

The material properties of timber and masonry, determined according to the methodology described in section 2.2.1, are reported in Tables 2 and 3, respectively. The peak strength and stiffness of the mechanical anchors are reported in Table 4, along with the values referred to cracked C20/25 concrete provided by the producer for seismic action category C1 as an indication [22]. Because the anchors were tested after fastening them to a single brick, it should be noticed that the results are not fully comparable to producer's values due to the weak and brittle behaviour of bricks, caused by splitting, especially under shear loading. Additional investigations on the performance of mechanical anchors in masonry are recommended; given the extension of the whole experimental campaign, only a preliminary study of their response was conducted in this case, especially to gain a first insight into the axial capacity of the anchors, essential to guarantee the load transfer between floors' joists and out-of-plane walls, and to prevent their collapse.

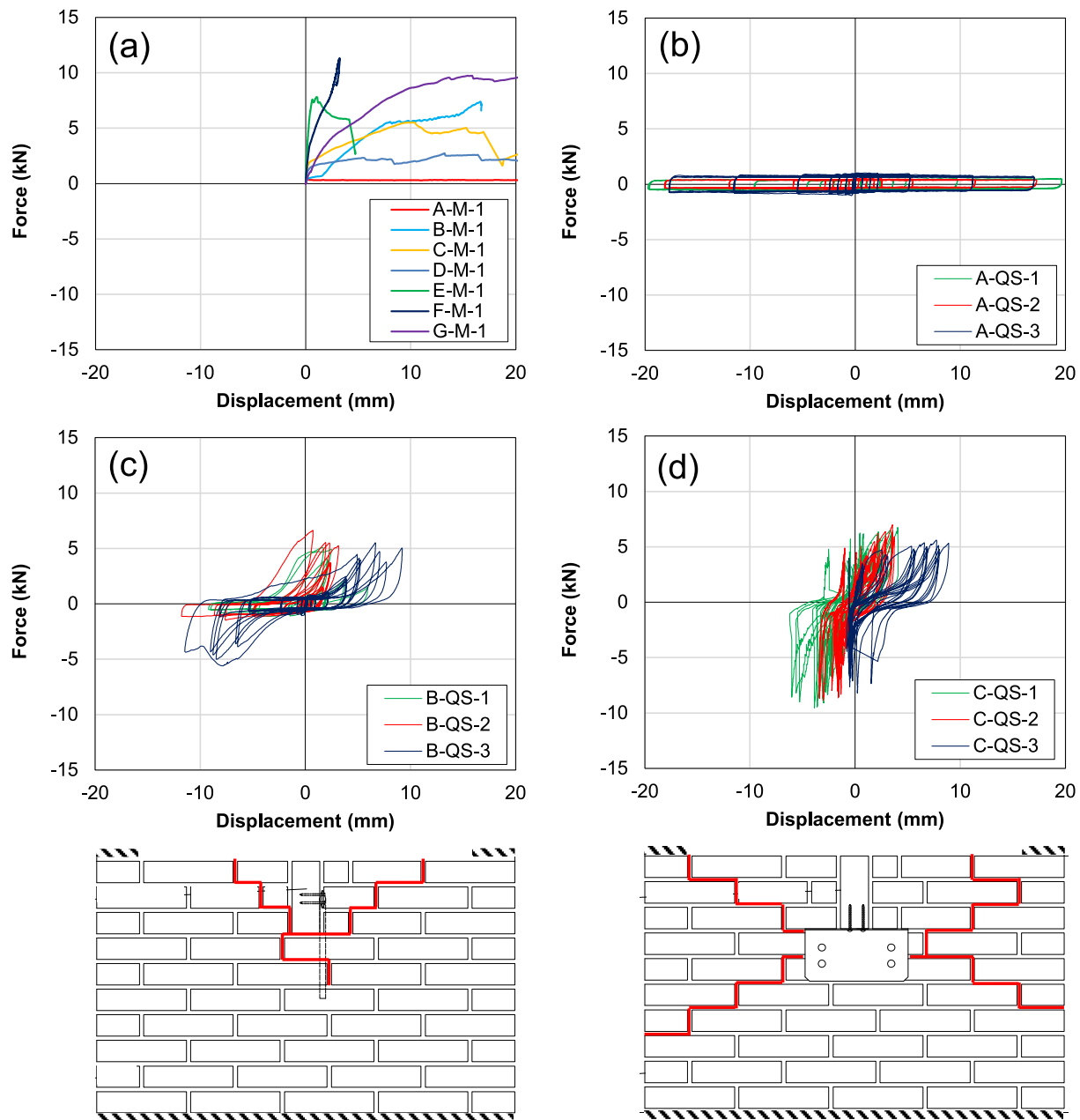


Fig. 6. Summary of monotonic (a) and cyclic test results for configurations A (b), B (c), C (d), D (e), E (f), F (g), G (h). For the configurations presenting damage on the masonry at the end of the test, a schematic representation of the typical crack pattern observed is also shown.

3.2. Quasi-static monotonic and cyclic tests on timber-masonry connections

The response under monotonic and quasi-static reversed-cyclic loading is shown in Fig. 6 for all configurations. The reported displacement is the joist-wall one, recorded by sensor 3. From monotonic tests (Fig. 6a), the difference in terms of stiffness and ductility among the seven tested configurations is already evident; these results are furtherly confirmed by the performed quasi-static cyclic tests, for which the typical crack pattern after testing is also shown for the configurations where damage on the masonry was observed. For a more comprehensive representation and discussion of failure modes, the reader is referred to Section 4.2.

Configuration A (Fig. 6b) showed a purely frictional behaviour and a very low force transfer between joist and wall, as expected. The strength

might be increased by the tilting of the joist in the mortar pocket (as observed for sample A-QS-3). The timber-mortar friction coefficient was quantified as $0.6 \div 0.8$. No cracks on the wall were present at the end of the test.

Configuration B also showed a frictional behaviour when pushing the connection, because the hook anchor was free to move, while in the opposite loading direction the wall was also involved in the resisting process, triggered by the vertical part of the anchor. It is interesting to notice that a reasonably high strength can be achieved even by an as-built configuration, although in one of the two loading directions only. As a last remark, sample B-QS-3 showed a more symmetric response because, after the first initial cycles with frictional behaviour in the pushing direction, a mortar particle detached from the pocket and remained clamped between the anchor and the wall, causing an increase in the transferred load (Fig. 6c).

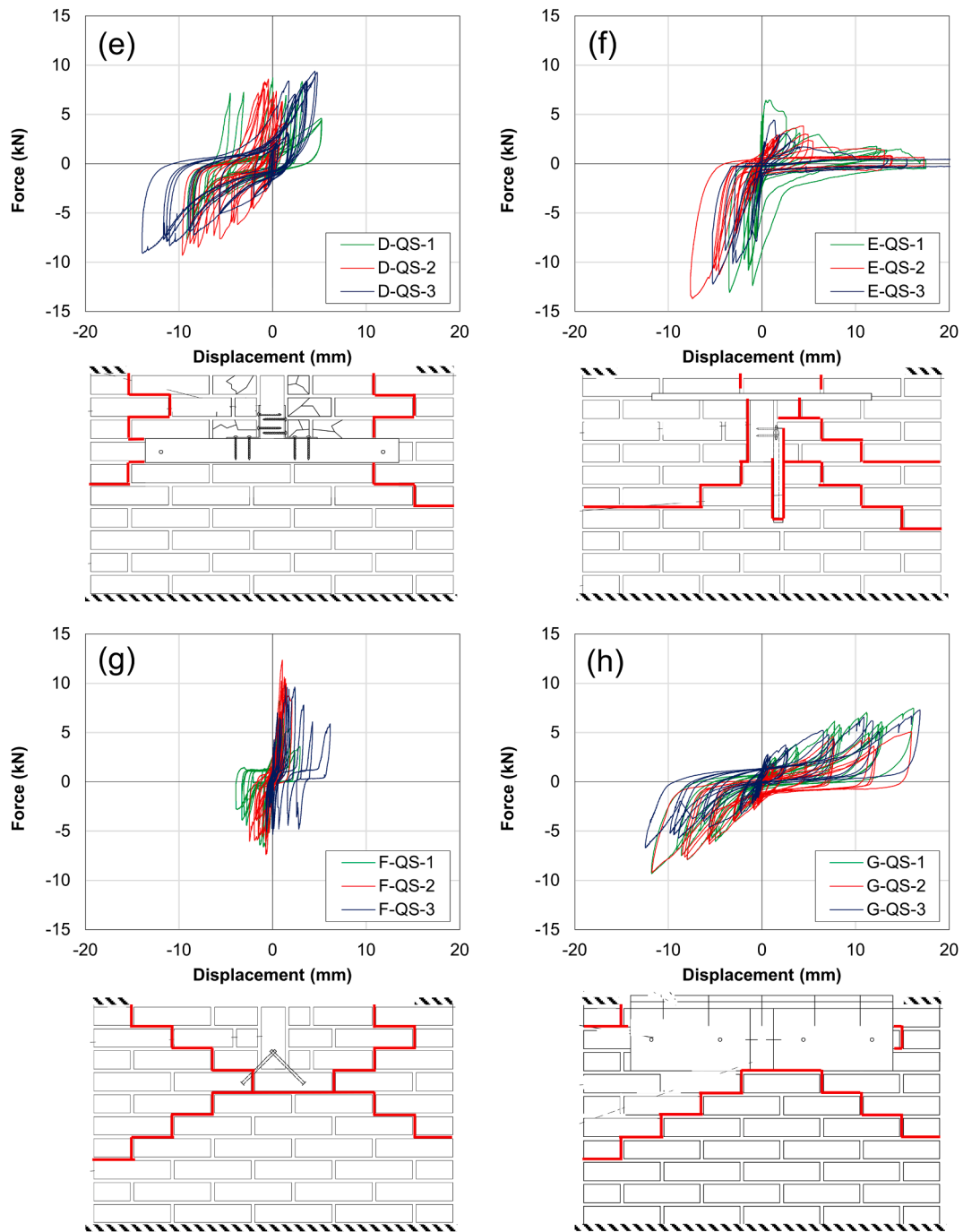


Fig. 6. (continued).

Configuration C represented a good compromise between strength and ductility. With this first retrofitting method, the capacity was increased more than tenfold compared to configuration A. The main failure modes were related to moderate yielding of the screws, together with bricks' or anchors' extraction from the wall, which displayed many cracks after testing (Fig. 6d). In the initial phases a quite uniform behaviour among the three tested configurations was observed.

Configuration D (Fig. 6e) displayed moderately high values of strength and stiffness, especially when considering that this option was applied to the walls of configuration B already damaged by the testing. Bending and yielding of screws and steel brackets were observed, and cracks on the walls occurred as well for very large displacements, leading to a non-symmetric behaviour. Depending on the larger or smaller play in all components of this connection type, a scatter in

stiffness was observed during the initial cycles.

Configuration E was developed in order to obtain a very stiff connection, even if not ductile. This objective was appropriately reached, as can be noticed from Fig. 6f. The initial response was uniform, with the exception of sample E-QS-2 that was, however, already slightly cracked around the connection. The main failure mode was the detachment from the wall of the glued part of the hook anchor, with also limited yielding of the nails connecting it to the joist. It should be noticed that the failure was not related to the glue itself, but to the cracking of bricks and mortar around it.

Configuration F was designed with the same purpose as option E. In this case, even more strength was achieved because of the efficient load transfer between joist and wall, and the three specimens exhibited in general a very similar response (Fig. 6g). No failure of screws and timber

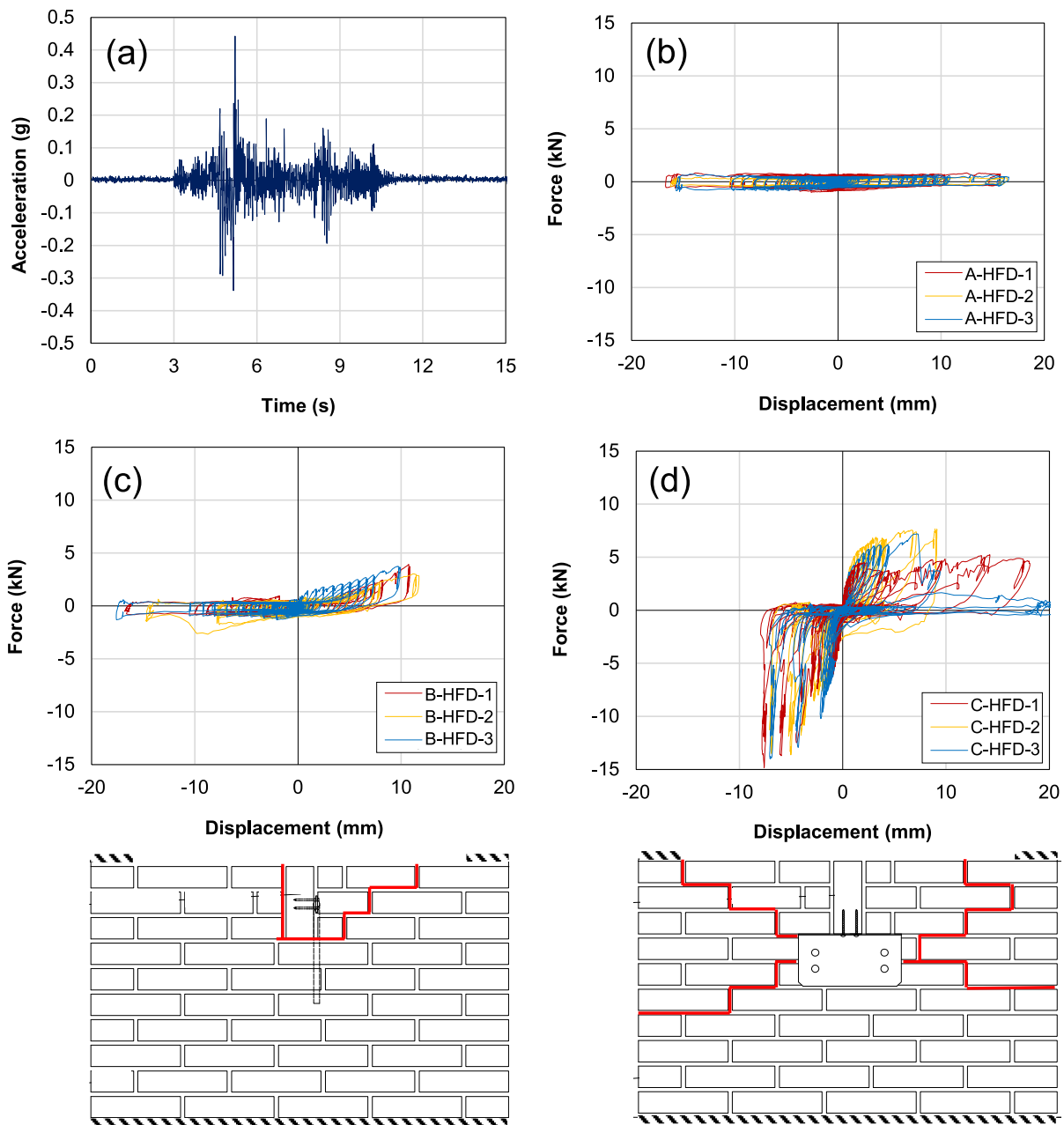


Fig. 7. Example of acceleration response measured at 100% signal amplitude on sample G-HFD-1 (a); dynamic test results for configurations A (b), B (c), C (d), D (e), E (f), F (g), G (h). For the configurations presenting damage on the masonry at the end of the test, a schematic representation of the typical crack pattern observed is also shown.

joint was observed, but a large and distributed crack pattern was visible in the tested samples.

Configuration G was instead developed to be a dissipative option, and this aim was properly achieved: the specimens showed high strength linked with ductility and energy dissipation, due to yielding and bending of screws and nails and, for large displacements, also cracking in the walls. Furthermore, the three tested samples displayed very similar hysteretic cycles, in both initial and overall behaviour (Fig. 6h).

3.3. Dynamic tests on timber-masonry connections

Similarly to quasi-static cyclic tests, Fig. 7 shows the hysteretic cycles obtained with the incremental dynamic tests for all samples. As a general remark, the load–displacement response of the specimens under a short

sudden earthquake loading did not largely differ from that of the quasi-statically tested ones. However, an impact effect was noticed especially in the pushing loading direction, increasing the capacity of the strengthened joints, or the play present in them. Furthermore, all samples appeared to be less damaged than those subjected to the quasi-static cyclic tests, probably because of the larger number of cycles performed in the latter case. These outcomes are discussed in more detail in Section 4.

Fig. 7a shows an example of the acceleration signal applied to the connection, selected to replicate the seismic motions that take place in Groningen, characterised by a short duration shock. The acceleration, recorded by the accelerometers on the connection, represents the 100 % of the reference signal (10 mm displacement amplitude).

Configuration A (Fig. 7b) displayed a behaviour very similar to that

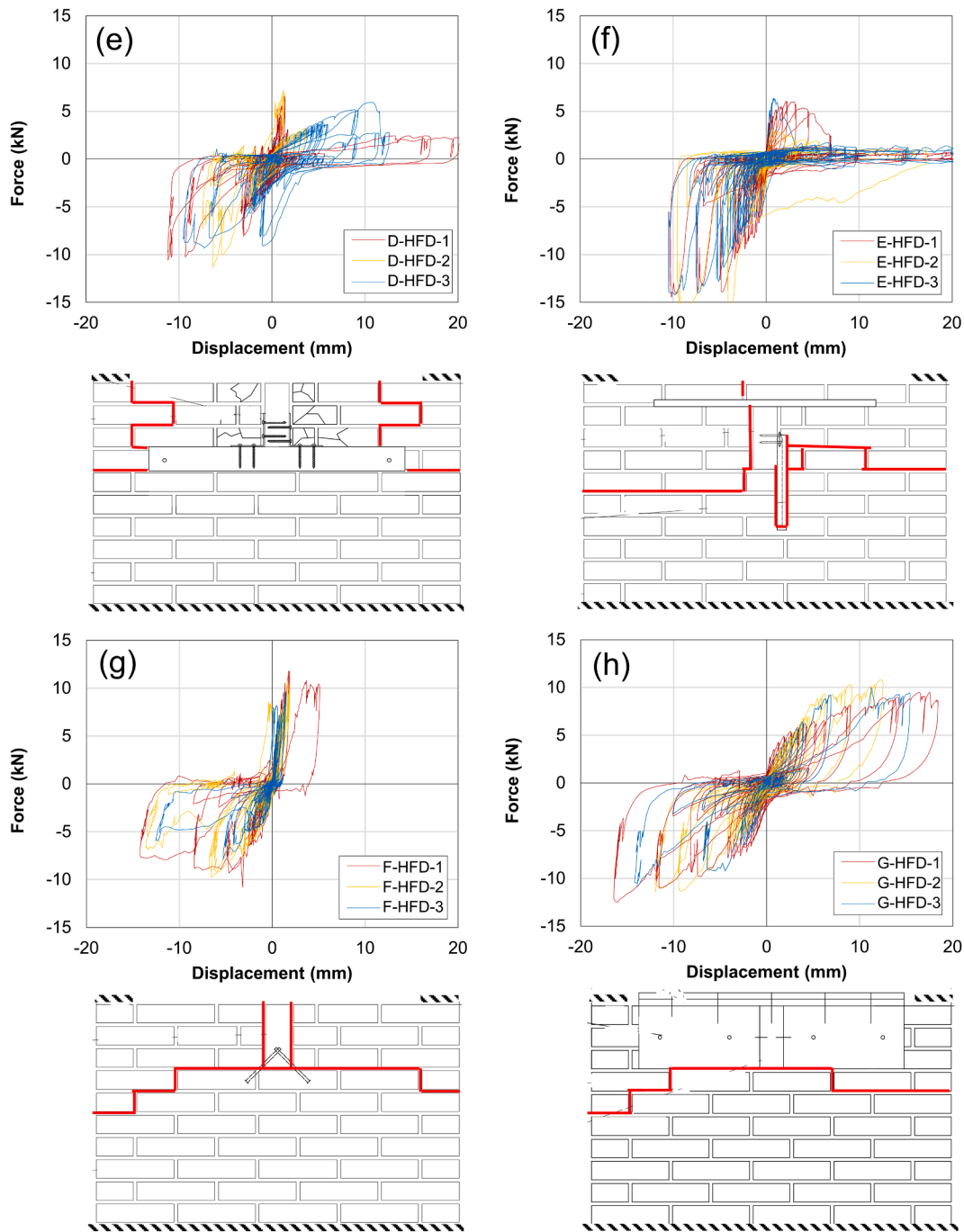


Fig. 7. (continued).

of the quasi-static tests; slightly higher forces were transferred by the joint, but in general the response was again frictional.

Configuration B (Fig. 7c) showed a frictional behaviour when pulling the connection, as it was observed for quasi-static tests, and an increase in strength when pushing the anchor. However, this increase occurred more gradually compared to the quasi-static cyclic response, probably because of the higher play in the connection induced by sudden loading.

Configuration C (Fig. 7d) exhibited a response equivalent to that measured for the quasi-static loading for the pulling direction, but not for the pushing direction, in which higher peak forces were reached due to the aforementioned impact effect. The failure modes were also very similar, although less damage was observed in the samples subjected to the dynamic loading.

For configuration D (Fig. 7e) the same remarks apply as for

configuration C, yet it is also important to notice that a slightly more flexible and less resistant behaviour was observed when pulling the joint.

Configuration E (Fig. 7f) was also very similar in terms of response to the quasi-static test results, but the impact effect when pushing determined once more higher peak forces in this loading direction.

Configuration F (Fig. 7g) showed higher force transfer when pushing as well; interestingly, under dynamic loading this connection type became approximately symmetric in terms of peak forces and stiffness. This behaviour could be explained considering that the load transfer is slightly less efficient in pushing, as observed in quasi-static cyclic tests, and this is counterbalanced by the impact effect in dynamic tests.

Configuration G (Fig. 7h) showed the same hysteretic behaviour as the one in quasi-static tests, but higher loads in both directions were

Table 5
Comparison between quasi-static and dynamic tests in terms of peak force in pulling and pushing, and stiffness evaluated at 2 mm displacement.

Configuration	Peak force in pulling (kN)		Peak force in pushing (kN)		Secant stiffness at 2 mm displacement (kN/mm)	
	QS tests	HFD tests	QS tests	HFD tests	QS tests	HFD tests
A	0.7 ± 0.3	0.6 ± 0.2	0.7 ± 0.3	0.8 ± 0.3	0.4 ± 0.2	0.3 ± 0.1
	5.8 ± 0.8	3.5 ± 0.5	1.2 ± 0.2	1.6 ± 0.9	0.5 ± 0.1	0.5 ± 0.2
C	6.4 ± 0.7	6.7 ± 1.3	8.9 ± 0.7	14.1 ± 0.6	2.6 ± 0.4	3.3 ± 0.3
	8.9 ± 0.4	5.6 ± 1.8	8.7 ± 0.9	10.4 ± 1.0	1.6 ± 0.6	1.9 ± 0.5
E	4.9 ± 1.4	5.2 ± 1.8	11.6 ± 2.4	14.8 ± 0.7	2.8 ± 1.2	2.9 ± 0.7
	10.1 ± 2.1	10.7 ± 1.1	6.4 ± 1.1	9.5 ± 1.5	3.6 ± 0.1	4.3 ± 0.4
G	6.6 ± 1.3	10.1 ± 0.7	8.4 ± 1.5	11.6 ± 0.9	1.4 ± 0.2	2.4 ± 0.2

reached. The overall dissipative and ductile behaviour was therefore again present, but with an improved transfer of force in the connection. Besides the aforementioned impact effect, a possible explanation for the higher peak strength in both loading directions could be the lower damage occurred on the top part of the masonry walls, compared to quasi-static tests.

4. Discussion

4.1. Comparison between quasi-static cyclic and dynamic tests

Table 5 shows a comparison between quasi-static and dynamic tests in terms of peak force measured for pulling and pushing forces, as well as of secant stiffness evaluated at 2 mm displacement. In this way, the large scatter in stiffness of the very initial cycles could be mitigated, while still obtaining values representative for the joints' linear elastic behaviour. As can be noticed, at least for short-duration shallow earthquakes such as the ones in Groningen, quasi-static tests can be considered reliable for assessing the response of connections similar to those investigated in this study: tests with such loading protocol are in general slightly more conservative, even if they cannot show phenomena such the impact effect or the higher play (and therefore a more flexible behaviour, as

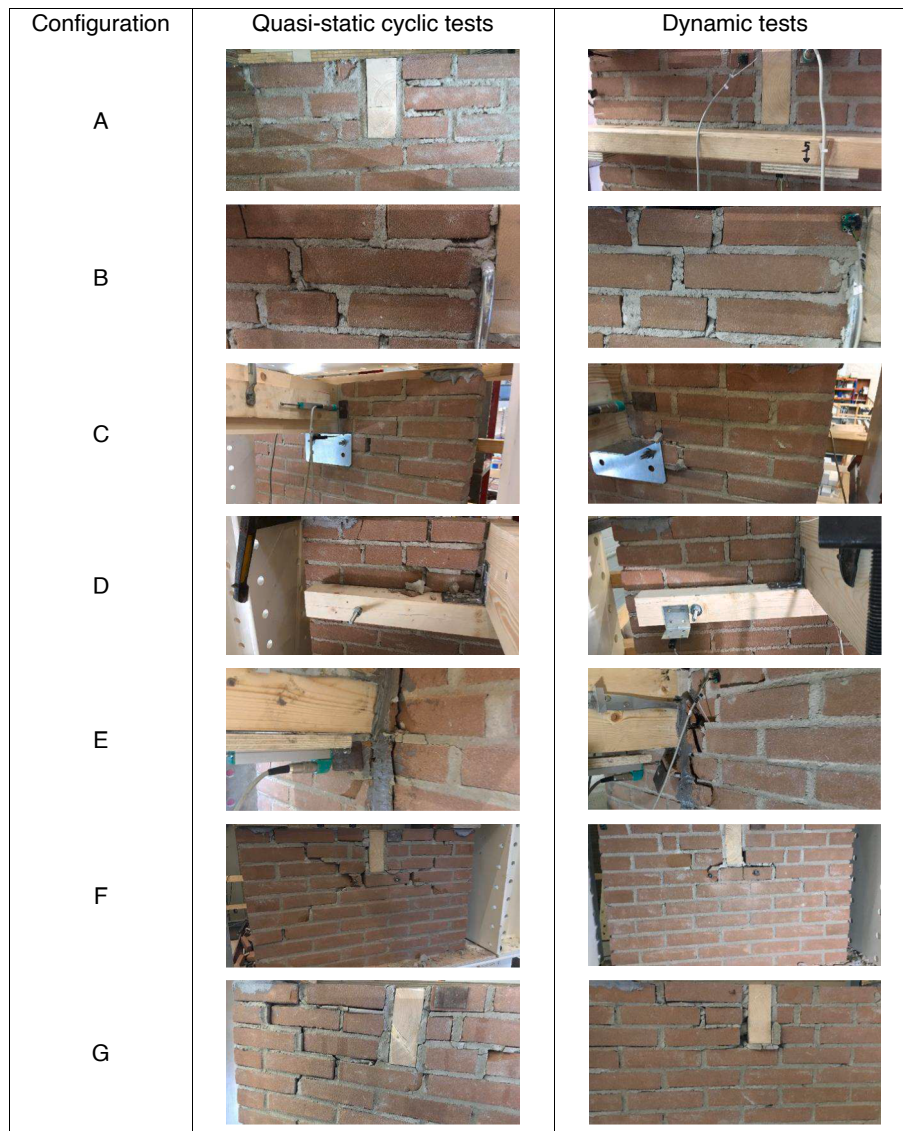


Fig. 8. Visual comparison of damage and cracks occurred to the walls under quasi-static cyclic and dynamic loading after the tests.

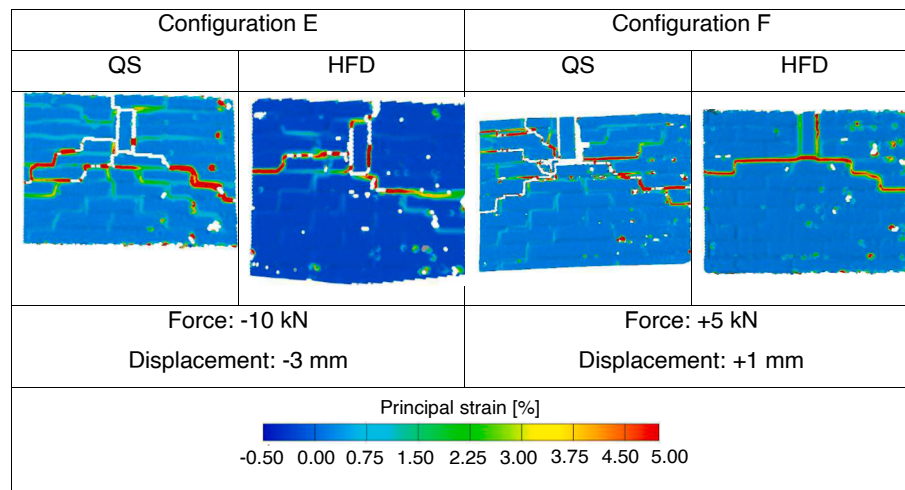


Fig. 9. Comparison of crack pattern under the same displacement amplitude at peak strength detected by DIC for configurations E and F in quasi-static cyclic and dynamic tests.

observed in configurations B and D) induced by the sudden loading in the connection.

The reason for the generally higher strength values obtained with the high-frequency dynamic tests could be related to the lower number of cycles applied to the connections in comparison to quasi-static cyclic tests. This fact could also explain the more limited damage on the walls, despite the sudden dynamic loading. To further investigate these aspects, firstly the crack pattern developed at peak force was compared, which for options E and F was also recorded with DIC in quasi-static and dynamic tests. Secondly, a long-duration tectonic earthquake signal (Irpinia, Italy, 1980 [26]) was applied to an additionally built sample representing configuration C: a different and longer dynamic loading representative of a tectonic earthquake was expected to cause way more damage compared to an induced earthquake's one.

As regards the crack pattern, a simple visual inspection of the samples (Fig. 8) already showed that the walls were less damaged when subjected to the induced earthquake loading with respect to the quasi-static tests (at the same displacement amplitude). This is confirmed with the more detailed information on cracks opening retrieved from DIC for options E and F (Fig. 9): this technique enabled to detect also the presence of very small cracks, otherwise not visible, which appeared to be way more spread in the samples' surface during quasi-static tests. This additional piece of information is of importance, confirming once more that quasi-static tests can be regarded as conservative for evaluating the response of the tested connections. Besides, according to the obtained results, masonry buildings in the Groningen area could undergo much less damage, compared to seismic regions subjected to relevant tectonic earthquakes.

To gain more insight into this last aspect, it was decided to take advantage of the versatility of the test setup: an additional sample with configuration C was constructed, and then subjected to the Irpinia earthquake signal (1980), having a much longer duration compared to that of the adopted induced signal from Groningen (86 s vs 14 s). The Irpinia signal was scaled to the same amplitude as the induced one, to have a consistent comparison. As can be noticed from Fig. 10a-b, the initial hysteretic behaviour of the connection under the tectonic earthquake signal was similar to the one recorded with the induced ground motion; however, the negative peak load dropped from 15 to 10 kN, thus a value closer to those observed during quasi-static tests (although this additional experiment is a single test and possibly not fully representative). Much more extensive damage was observed on the sample subjected to the tectonic earthquake, which almost collapsed during the last run (Fig. 10d), although subjected to the same displacement amplitudes in each run. A less evident impact effect was also present, due to the

slightly lower frequency of the tectonic signal compared to the induced one.

The proposed retrofitting options could greatly improve the seismic response of the building stock in the Groningen area: not only at structural level, by providing a box-like behaviour, but also at material level, with a lower damage underwent by the masonry, and even a dissipative contribution of the connections, discussed in section 4.3.

4.2. Failure modes

In this section, the possible failure modes of the joints are discussed. Not all the failure modes discussed below were observed during the tests, but they are included because they may occur in presence of more deteriorated structural elements and materials. Fig. 11 displays a summary of the tested configurations with the relative failure modes and the description of the main outcomes from the tests.

With regard to as-built configurations, the frictional behaviour of joint type A does not lead to a real failure mode with damage at connection level. At structural level, a detachment of the wall from the joists could occur instead, with the consequent out-of-plane collapse of the wall. This same consideration applies for configuration B in the pushing direction, while the presence of the hook anchor may cause cracking in the masonry and yielding of nails when pulling, as observed during the performed tests. Because very frequently this joint type features large-diameter nails, it can be expected that the governing failure mechanism in pulling is cracking of masonry, with the total strength depending on the extension of the portion of wall activated by the hook anchor.

When considering the strengthened configurations, a larger number of failure mechanisms can occur for the same configuration. In configuration C and D, bending and yielding of screws and steel angles were observed, as well as cracks in the walls around the joints. For large displacements, and not in all cases, the pull-out failure of one mechanical anchor occurred as well. Especially for configuration C, the latter mechanism could explain why the obtained value of ultimate load (≈ 7 kN) was lower than the total strength of the four applied screws (≈ 8 kN according to the data of the supplier). Thus, with more extended investigations on the strength and performance of mechanical anchors in masonry, such joint detail could be optimized to achieve capacity design, firstly enabling full yielding of screws, prior to pull-out failure of anchors. This same recommendation applies for configuration D, even if for this case the ultimate load (≈ 9 kN) was in line with the strength of ≈ 8 kN expected for the applied screws.

Configuration E was characterized by yielding of the nails connecting

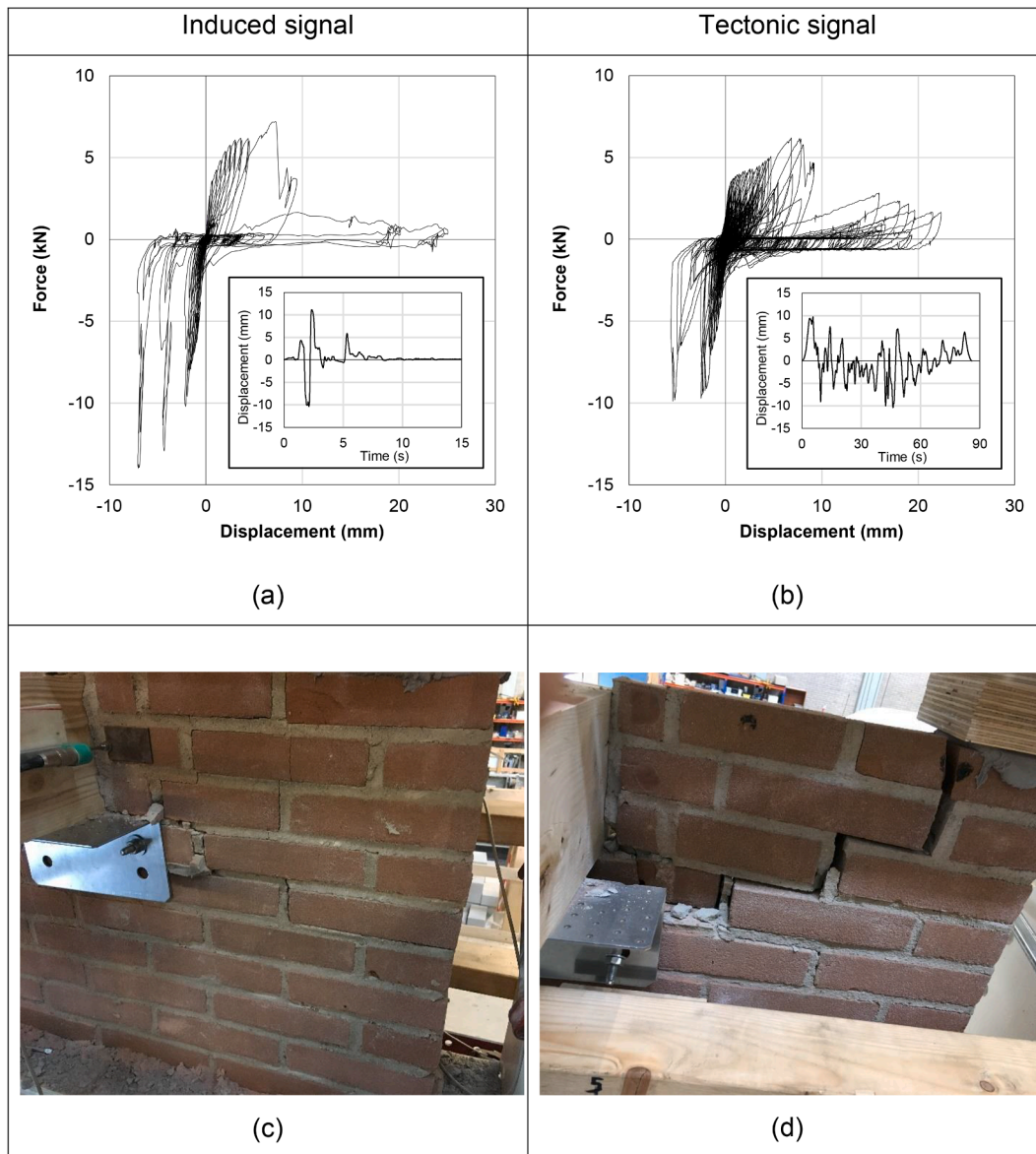


Fig. 10. Comparison between the connections' hysteretic cycles obtained with induced (a) and tectonic signal (b); the displacement time-history applied by the actuator is also shown; damage on the walls and the connection after the tests with induced (c) and tectonic signal (d).

the hook anchor to the joist and by the detachment of the glued interface from the wall, a brittle and less desirable failure mode. Moreover, cracks on the walls were also detected. In configuration F, the main failure mode was related to the damage on the walls and the brick sliding or extraction due to the screws' action. Ideally, also bending and yielding of the screws could potentially occur, but they were not observed during the performed tests due to the large diameter adopted for the screws. Because of the specific failure mechanism observed, the strength of this joint type could be estimated based on the weight acting on the connection, on the shear strength and friction coefficient, and on the area of the masonry portion activated by the screws. For this case, these parameters are 0.5 kN, 0.15 MPa, 0.78, and $420 \times 100 \text{ mm}^2$, respectively, providing a strength of $0.15 \times 42000 + 0.78 \times 500 = 6.7 \text{ kN}$, very close to the average 6.4 kN value measured in the pushing direction.

Finally, for configuration G, yielding of nails and screws was noticed, together with cracks on the walls and, for very large displacements, the pull-out failure of one or two mechanical anchors. Therefore, also for this case and especially in quasi-static tests, the recorded ultimate load was influenced by extraction of mechanical anchors, leading to $\approx 7 \text{ kN}$ in place of the expected total strength of $\approx 8 \text{ kN}$ referred to the applied

screws.

More detailed calculation models can be set up for each failure mode, and will be investigated more in depth in future works.

4.3. Dissipative properties of the tested connections

Finally, the possible beneficial, dissipative effect of the tested timber-masonry connections was investigated. The energy dissipation provided by each configuration was quantified in terms of an equivalent damping ratio ξ , evaluated at the cycle corresponding to half of the peak force. For configuration A, for which the peak force was constant due to the frictional response, ξ was evaluated at half of the maximum applied displacement. The damping ratios were calculated by adopting the energy loss per cycle method [27]; since the hysteretic responses were retrieved from the combination of the force transferred by the connections, measured by the load cell on the timber joist, and sensor 3, measuring the relative displacement between joist and wall (see Section 2.2.2 and Fig. 4), the calculated ξ values can be regarded as a fair estimation of the energy dissipated in the joints. The results of this analysis are reported in Table 6.






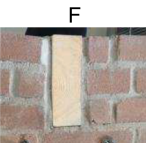

Joint type	Failure mechanisms	Remarks from quasi-static tests	Remarks from dynamic tests
<p>A</p> 	<p>Friction on the joist-mortar interface</p>	<p>Frictional response</p>	<p>Higher strength values due to sudden load relatively to quasi-static tests, but absolute strength values still low</p>
<p>B</p> 	<ul style="list-style-type: none"> • Friction on the joist-mortar interface • Yielding of nails • Cracking of masonry 	<p>Whole wall activated in pulling after frictional behaviour</p>	<p>Higher play and lower stiffness</p>
<p>C</p> 	<ul style="list-style-type: none"> • Yielding of screws • Cracking of masonry or bricks' extraction • Bending and yielding of the steel angle • Pull-out failure of the mechanical anchors 	<p>Whole wall activated in both directions with effective transfer of load; yielding of screws and steel angle</p>	<p>Same stiffness, higher pushing strength due to impact effect</p>
<p>D</p> 	<ul style="list-style-type: none"> • Yielding or pull-out failure of screws • Cracking of masonry or bricks' extraction • Bending and yielding of the steel brackets • Pull-out failure of the mechanical anchors 	<p>Whole wall activated in both directions with effective transfer of load; yielding of screws and angle brackets</p>	<p>Higher play, lower stiffness; lower pulling strength and higher pushing strength due to impact effect</p>
<p>E</p> 	<ul style="list-style-type: none"> • Yielding of nails • Cracking of masonry • Detachment of glue pocket with extraction of the hook anchor 	<p>Whole wall activated in both directions with effective transfer of load until detachment of glued interface</p>	<p>Slightly higher pushing strength due to impact effect</p>
<p>F</p> 	<ul style="list-style-type: none"> • Cracking of masonry or bricks' extraction • <i>Yielding or pull-out failure of screws</i> 	<p>Whole wall activated in both directions with effective transfer of load and a very stiff behaviour</p>	<p>Higher play and lower stiffness, higher strength</p>
<p>G</p> 	<ul style="list-style-type: none"> • Yielding or pull-out failure of screws and nails • Cracking of masonry or bricks' extraction • Pull-out failure of the mechanical anchors 	<p>Whole wall activated in both directions with effective transfer of load and with a very ductile behaviour</p>	<p>Slightly higher strength and stiffness</p>

Fig. 11. Summary of the possible failure modes (in italic those not observed in the tests, but possible in practice) and main outcomes from the tests for each connection type.

Configuration A showed the highest damping value because of its frictional behaviour and displacement capacity, but its limited shear transfer would not be sufficient to prevent the walls from out-of-plane collapses. For this reason, when this component is evaluated as part of

a whole building, its performance would be insufficient. The values determined for the other connections show two distinct groups: configurations B, C, D and G, thus the most ductile ones, exhibited remarkable damping values, besides improving the stiffness and

Table 6

Equivalent damping ratio values at the cycle corresponding to half of peak force for all tested configurations.

Configuration	Equivalent damping ratio ξ evaluated at half of peak force
A	0.59 ± 0.03
B	0.23 ± 0.03
C	0.20 ± 0.08
D	0.23 ± 0.05
E	0.08 ± 0.02
F	0.14 ± 0.02
G	0.18 ± 0.03

strength of the as-built configurations. Connection types E and F showed lower ξ values because these strengthening methods privileged strength and stiffness rather than energy dissipation, which is mainly provided by wall's cracking.

5. Conclusions

This work presented an experimental campaign which aimed at characterizing the response of as-built and strengthened timber masonry connections. For a comprehensive evaluation of the joints' behaviour, three test types were conducted, namely quasi-static monotonic and reversed cyclic, and dynamic. The obtained test results showed that it was possible to increase largely the strength and stiffness of the as-built configurations via the application of retrofitting and strengthening measures. For the solutions designed to have a ductile behaviour, also high energy dissipation was achieved.

The conducted experimental characterisation provided the following outcomes:

- In presence of a mortar pocket (configuration A), a friction coefficient of $0.6 \div 0.8$ was derived. This value can be taken into account when performing seismic assessment of existing buildings with such timber-masonry connections.
- The second tested as-built-configuration (B, hook anchor inserted in the masonry and nailed to the joist), widespread in the building stock of the province of Groningen, presented a non-symmetric response because of the shape of the hook anchor. The behaviour is frictional in pushing, whereas in pulling higher strength can be retrieved, but only at a large amount of slip. Since in practice this joint type features nails (whose strength can be estimated e.g. with Eurocode 5) having a large diameter, the governing failure mechanism in pulling is cracking of masonry, with the total strength depending on the extension of the portion of wall activated by the hook anchor.
- Configuration C (joint retrofitted with a steel angle screwed to the joist and anchored to the masonry) showed a great increase in strength compared to as-built joints. The obtained value of ultimate load was slightly lower than the total strength of the four applied screws, because of the incipient extraction of a mechanical anchor or a full brick in the final phases of the tests. In order to achieve a proper capacity design of the joint, with sufficiently over-resistant mechanical anchors with respect to screws, further experiments are recommended to characterize in detail their performance in terms of strength and stiffness in masonry walls.
- Configuration D (joint retrofitted with an additional timber beam screwed to the existing joist and anchored to the masonry) showed a capacity comparable to configuration C: this result is promising, as this connection type was applied to masonry already damaged around the joist. For this case, the ultimate load was more in line with the strength expected for the applied screws. However, the aforementioned recommendation on the evaluation of the performance of mechanical anchors in masonry applies, as also for this configuration a partial extraction of few of them at the end of the tests was observed.

- Configuration E (joint retrofitted with hook anchor embedded in epoxy) potentially allows the reuse of existing hook anchors and creates a very stiff connection. However, the behaviour recorded in the pulling direction was very brittle, with a sudden failure of the masonry around the epoxy. Further investigations are recommended on the evaluation of the strength at the interface between epoxy and masonry, in order to achieve in full a capacity design of the whole joint.
- Configuration F (joint retrofitted with two inclined screws embedded in epoxy and crossing the wall) also constitutes a very stiff retrofitting option, providing a stable cyclic behaviour. In this case, the ultimate load was reached when extraction of bricks occurred, a mechanism linked to shear failure in the mortar joint, based on which the strength of the connection can be estimated.
- Finally, configuration G (joint retrofitted with timber blocks anchored to the masonry and connected to existing joist and sheathing) showed great strength and ductility. Also for this case, the recorded ultimate load was influenced by extraction of mechanical anchors, leading to a slightly lower strength than that of the applied screws. Once more, the aforementioned recommendation on the evaluation of the performance of mechanical anchors in masonry applies.

With reference to the applied testing protocols, quasi-static tests proved to be reliable and conservative for characterizing timber-masonry connections with Dutch features, also in the context of structures subjected to induced earthquakes, for which the performed dynamic tests showed that the damage on both joints and masonry is more limited than that observed for quasi-static cyclic tests. Furthermore, load duration and number of cycles of the loading protocol have a relevant effect on the performance of the connection: when the loading protocol was based on a tectonic earthquake, way more extended damage was observed than that obtained for a signal representative of an induced earthquake, and more similar to the one recorded in quasi-static tests.

The obtained results constitute a further step towards the knowledge of material properties and the correct seismic assessment of timber-masonry connections for the Dutch building stock. Moreover, they provide input values for numerical models, enabling additional studies and sensitivity analyses on this topic. Further research is ongoing to formulate design suggestions and study the behaviour of these joints at structural level, mainly in terms of impact of the single strengthening interventions on the response of whole buildings.

CRedit authorship contribution statement

Michele Mirra: Conceptualization, Methodology, Formal analysis, Investigation, Data curation, Writing – original draft, Visualization. **Geert Ravenshorst:** Conceptualization, Methodology, Investigation, Writing – review & editing, Supervision, Project administration, Funding acquisition. **Peter de Vries:** Conceptualization, Methodology, Investigation, Writing – review & editing, Supervision, Project administration. **Francesco Messali:** Methodology, Investigation, Writing – review & editing, Supervision, Project administration, Funding acquisition.

Declaration of Competing Interest

The authors declare that they have no known competing financial interests or personal relationships that could have appeared to influence the work reported in this paper.

Data availability

Data will be made available on request.

Acknowledgements

The Authors thankfully acknowledge NAM (Nederlandse Aardolie Maatschappij) for having funded this experimental campaign (grant no. CS2B04), Rothoblaas for having provided the screws and the epoxy, and the whole staff of Stevin II Laboratory at TU Delft, for their precious help during the construction and testing phase.

References

- [1] T. van Eck, F. Goutbeek, H. Haak, B. Dost, Seismic hazard due to small-magnitude, shallow-source, induced earthquakes in The Netherlands, *Eng. Geol.* 87 (2006) 105–121.
- [2] F. Messali, G. Ravenshorst, R. Esposito, J.G. Rots, Large-scale testing program for the seismic characterization of Dutch masonry walls. Proceedings of 16th World Conference on Earthquake (WCEE), 2017. Santiago, Chile.
- [3] S. Jafari, J.G. Rots, R. Esposito, F. Messali, Characterizing the Material Properties of Dutch Unreinforced Masonry, *Procedia Eng.* 193 (2017) 250–257.
- [4] R. Esposito, F. Messali, G.J.P. Ravenshorst, H.R. Schipper, J.G. Rots, Seismic assessment of a lab-tested two-storey unreinforced masonry Dutch terraced house, *Bull. Earthq. Eng.* 17 (8) (2019) 4601–4623.
- [5] F. Messali, R. Esposito, G.J.P. Ravenshorst, J.G. Rots, Experimental investigation of the in-plane cyclic behaviour of calcium silicate brick masonry walls, *Bull. Earthq. Eng.* 18 (8) (2020) 3963–3994.
- [6] M. Mirra, G. Ravenshorst, J.-W. van de Kuilen, Experimental and analytical evaluation of the in-plane behaviour of as-built and strengthened traditional wooden floors, *Eng. Struct.* 211 (2020), 110432.
- [7] M. Mirra, G. Ravenshorst, J.-W. van de Kuilen, Comparing in-plane equivalent shear stiffness of timber diaphragms retrofitted with light and reversible wood-based techniques, *Pract. Period. Struct. Des. Constr.* 26 (4) (2021).
- [8] M. Mirra, G. Ravenshorst, P. de Vries, J.-W. van de Kuilen, An analytical model describing the in-plane behaviour of timber diaphragms strengthened with plywood panels, *Eng. Struct.* 235 (2021), 112128.
- [9] M. Mirra, M. Sousamli, M. Longo, G. Ravenshorst, Analytical and numerical modelling of the in-plane response of timber diaphragms retrofitted with plywood panels. 8th International Conference on Computational Methods in Structural Dynamics and Earthquake Engineering, COMPDYN 2021, Athens, Greece, 2021.
- [10] M. Mirra, G. Ravenshorst, Optimizing seismic capacity of existing masonry buildings by retrofitting timber floors: wood-based solutions as a dissipative alternative to rigid concrete diaphragms, *Buildings* 11 (12) (2021) 604.
- [11] T.-J. Lin, J.M. LaFave, Experimental structural behavior of wall-diaphragm connections for older masonry buildings, *Constr. Build. Mater.* 26 (2012) 180–189.
- [12] S. Moreira, D.V. Oliveira, L.F. Ramos, P.B. Lourenço, R.P. Fernandes, J. Guerreiro, Experimental study on the seismic behavior of masonry wall-to-floor connections. 15th World Conference on Earthquake Engineering, Lisbon, Portugal, 2012.
- [13] S. Moreira, L.F. Ramos, D.V. Oliveira, P.B. Lourenço, L. Mateus, Developing a seismic retrofitting solution for wall-to-floor connections of URM with wood diaphragms. 9th International Masonry Conference, Guimarães, Portugal, 2014.
- [14] D. Dizhur, M. Giaretton, J. Ingham, URM wall-to-diaphragm and timber joist connection testing. 10th International Masonry Conference, Milan, Italy, 2018.
- [15] EN 338 – Structural timber—Strength classes. CEN (European Committee for Standardization). 2009, Brussels, Belgium.
- [16] EN 13183-1:2002. Moisture content of a piece of sawn timber – Part 1: Determination by oven dry method. CEN (European Committee for Standardization).
- [17] G.J.P. Ravenshorst, J.W.G. Van de Kuilen, Relationships between local, global and dynamic modulus of elasticity for soft- and hardwoods. CIB W18, proceedings paper 42-10-1, Dubendorf, Switzerland, 2009.
- [18] EN 1015-11:1999. Methods of test for mortar for masonry – Part 11: Determination of flexural strength of hardened mortar. CEN (European Committee for Standardization).
- [19] EN 1052-1:1998. Methods of test for masonry – Part 1: Determination of compressive strength. CEN (European Committee for Standardization).
- [20] EN 1052-5:2005. Methods of test for masonry – Part 5: Determination of bond strength by bond wrench method. CEN (European Committee for Standardization).
- [21] EN 1052-3:2002. Methods of test for masonry – Part 3: Determination of initial shear strength. CEN (European Committee for Standardization).
- [22] European Technical Assessment ETA-05/0069. Deutsches Institut für Bautechnik, 24th April 2020.
- [23] EN 846-5:2012 – Methods of test for ancillary components for masonry. Determination of tensile and compressive load capacity and load displacement characteristics of wall ties.
- [24] ISO 16670:2003. Timber structures – Joints made with mechanical fasteners – Quasi-static reversed-cyclic test method. International Organization for Standardization (ISO).
- [25] M. Miglietta, L. Mazzella, L. Grottoli, G. Guerrini, F. Graziotti, Full-scale building test – EC build 6: test results report. Protocol number EUC160/2018, version 1.1, 31/07/2018.
- [26] P. Bernard, A. Zollo, The Irpinia (Italy) 1980 earthquake: detailed analysis of a complex normal faulting, *J. Geophys. Res.* 94 (1989) 1631–1647.
- [27] R.W. Clough, J. Penzien, Dynamics of structures, Computer & Structures Inc, 1995.